Asian Journal of Andrology (2019) 21, 365–374
www.asiaandro.com; www.ajandrology.com

Open Access

ORIGINAL ARTICLE

Sperm Biology

Regulation of blood-testis barrier dynamics by the mTORC1/rpS6 signaling complex: an *in vitro* study

Lin-Xi Li[1,2,*], Si-Wen Wu[1,2,*], Ming Yan[2,3], Qing-Quan Lian[1], Ren-Shan Ge[1], C Yan Cheng[1,2]

During spermatogenesis, developing germ cells that lack the cellular ultrastructures of filopodia and lamellipodia generally found in migrating cells, such as macrophages and fibroblasts, rely on Sertoli cells to support their transport across the seminiferous epithelium. These include the transport of preleptotene spermatocytes across the blood-testis barrier (BTB), but also the transport of germ cells, in particular developing haploid spermatids, across the seminiferous epithelium, that is to and away from the tubule lumen, depending on the stages of the epithelial cycle. On the other hand, cell junctions at the Sertoli cell–cell and Sertoli–germ cell interface also undergo rapid remodeling, involving disassembly and reassembly of cell junctions, which, in turn, are supported by actin- and microtubule-based cytoskeletal remodeling. Interestingly, the underlying mechanism(s) and the involving biomolecule(s) that regulate or support cytoskeletal remodeling remain largely unknown. Herein, we used an *in vitro* model of primary Sertoli cell cultures that mimicked the Sertoli BTB *in vivo* overexpressed with the ribosomal protein S6 (rpS6, the downstream signaling protein of mammalian target of rapamycin complex 1 [mTORC1]) cloned into the mammalian expression vector pCI-neo, namely, quadruple phosphomimetic and constitutively active mutant of rpS6 (pCI-neo/p-rpS6-MT) versus pCI-neo/rpS6-WT (wild-type) and empty vector (pCI-neo/Ctrl) for studies. These findings provide compelling evidence that the mTORC1/rpS6 signal pathway exerted its effects to promote Sertoli cell BTB remodeling. This was mediated through changes in the organization of actin- and microtubule-based cytoskeletons, involving changes in the distribution and/or spatial expression of actin- and microtubule-regulatory proteins.
Asian Journal of Andrology (2019) **21**, 365–374; doi: 10.4103/aja.aja_126_18; published online: 1 March 2019

Keywords: blood-testis barrier; F-actin; microtubule; mTORC1; rpS6; Sertoli cells; testis

INTRODUCTION

Mammalian target of rapamycin (mTOR), a Ser/Thr protein kinase known to regulate cellular energy status in virtually all mammalian cells,[1–4] is also a key signaling protein in the testis that supports spermatogenesis.[5,6] Studies have shown that when mTOR associates with the adaptor protein, regulatory-associated protein of mTOR (Raptor), or rapamycin-insensitive companion of mTOR (Rictor), they create either the mammalian target of rapamycin complex 1 (mTORC1) or the mTORC2 signaling protein, which have distinctive cellular functions to support epithelial homeostasis.[2,4,6,7] Studies in the testis have shown that mTORC1/protein ribosomal protein S6 (rpS6) signaling complex promotes Sertoli cell blood-testis barrier (BTB) remodeling, possibly being used to support the transport of preleptotene spermatocytes across the immunological barrier such as at late Stage VII through early Stage IX of the epithelial cycle in the rat testis by facilitating BTB restructuring.[8] Subsequent studies have shown that this is mediated via an activation of the mTORC1 signaling protein, rpS6,[9,10] downstream, through a surge in the expression of p-rpS6-S235/S236 and p-rpS6-S240/S244 in the testis, perturbing permeability barrier function of the Sertoli cell tight junction (TJ).[11] This was followed by a down-regulation of p-Akt1/2, through disruptive changes in the organization of actin-based cytoskeleton in studies *in vitro*.[11,12]

In this context, it is of interest to note that mTORC2, unlike mTORC1, exerts its regulatory effects at the BTB that promotes the immunological barrier integrity through connexin 43 (Cx43), involving an activation of protein kinase C alpha (PKCα) and Rac family small GTPase 1 (Rac1) downstream that modify the organization of actin-based cytoskeleton in Sertoli cells.[13] These findings are also consistent with earlier reports that Cx43 is necessary to maintain cross-talks between different junctions at the BTB (*e.g.*, actin-based TJ, basal ectoplasmic specialization [basal ES], and gap junction, as well as intermediate filament-based desmosome[14–18]) to maintain BTB homeostasis.[19,20] This involvement of mTOR in testis function via its effects on Sertoli cell cytoskeletal organization and the activation of rpS6 have since been confirmed in genetic models in mice.[21–25] In this context, we have prepared a quadruple phosphomimetic (and constitutively active) mutant of rpS6, namely, p-rpS6-MT by converting Ser in S235/S236 and S240/S244 (*i.e.*, p-rpS6-S235/S236/S240/S244) to Glu (E) (*i.e.*, p-rpS6-E235/E236/E240/E244) using site-directed mutagenesis by PCR as detailed elsewhere.[11,12] Overexpression of this p-rpS6-MT in primary Sertoli cells cultured *in vitro* with an established functional TJ-barrier has been shown to induce Sertoli cell BTB disruption *in vitro* through changes in the organization of F-actin across Sertoli cells.[11,12] More importantly, these

[1]The Second Affiliated Hospital and Yuying Children's Hospital, Wenzhou Medical University, Wenzhou 325027, China; [2]The Mary M. Wohlford Laboratory for Male Contraceptive Research, Center for Biomedical Research, Population Council, New York, NY 10065, USA; [3]Jiangsu Key Laboratory of Drug Screening, China Pharmaceutical University, Nanjing 210009, China.
*These authors contributed equally to the work.
Correspondence: Dr. CY Cheng (y-cheng@popcbr.rockefeller.edu) or Dr. QQ Lian (lianqingquanmz@163.com)
Received: 27 July 2018; Accepted: 18 December 2018

findings *in vitro* have recently been shown to be relevant to the testis *in vivo*, since overexpression of this quadruple phosphomimetic mutant rpS6-MT in the testis *in vivo* indeed perturbs the Sertoli cell BTB function through changes in the actin-based cytoskeletal function.[26] Since studies have shown that the microtubule-based cytoskeleton is intimately associated with the actin-based cytoskeleton to support Sertoli cell function, in particular at the apical and the basal ES (*i.e.*, at the Sertoli cell-cell interface at the BTB, and also the apical ES at the Sertoli-spermatid interface[14,27–31]), we thought it pertinent to examine if rpS6 also modulates the microtubule-based cytoskeletal organization at the Sertoli cell BTB and the underlying mechanism(s) of action. This information should be helpful to understand better the biology of mTORC1/rpS6/Ak transforming 1/2/(Akt1/2, also called protein kinase B or PKB) signaling pathway in regulating spermatogenesis.

MATERIALS AND METHODS

Animals

Male pups at 16–18 days of age were purchased from Charles River Laboratories (Kingston, NY, USA). Ten male pups with a foster mother rat were housed in the same cage at the Rockefeller University Comparative Bioscience Center (CBC; New York, NY, USA) in accordance with the applicable portions of the Animal Welfare Act and the guidelines in the Department of Health and Human Services publication *Guide for the Care and Use of Laboratory Animals*. These male pups, in groups of 10 pups per experiment, were used at 20 days of age for the isolation of Sertoli cells for primary cultures to provide enough Sertoli cells for an experiment consisting of different treatment and control groups. The use of animals for all experiments reported herein was approved by the Rockefeller University Institutional Animal Care and Use Committee (IACUC) with protocol numbers 15–780-H and 18-043-H. The use of LipoJet *In Vitro* DNA transfection reagent (SignaGen Lab, Rockville, MD, USA) for applicable *in vitro* experiments involving recombinant DNA material was approved by the Rockefeller University Institutional Biosafety Committee (IBC) with approval number 2-15-04-007. All rats were euthanized by CO_2 asphyxiation using slow (approximately 20%–30% min^{-1}) displacement of chamber air from compressed CO_2 in a euthanasia chamber with a built-in gas regulator approved by the Rockefeller University Laboratory Safety and Environmental Health (LSEH).

Antibodies

Antibodies and their Resource Identification Initiative (RRID) used for various experiments reported here were obtained from commercial vendors, unless otherwise specified, as noted in **Supplementary Table 1**. The working dilutions and specific applications were also listed.

Isolation and primary culture of Sertoli cells

Sertoli cells were isolated from testes of 20-day-old rats in a group of 10 male pups as described.[32] Freshly isolated Sertoli's cells were seeded on Matrigel (Fisher Scientific, Waltham, MA, USA)-coated culture dishes (either 6-, 12- or 24-well dishes), coverslips (to be placed in 12-well dishes), and bicameral units (Millipore, Burlington, MA, USA; to be placed in 24-well dishes) at a density 0.4×10^6–0.5×10^6, 0.03×10^6–0.04×10^6, and 1.0×10^6 cells per cm^2, respectively, in serum-free Nutrient Mixture F12/Dulbecco's Modified Eagle Medium (F12/DMEM; Gibco/Thermo Fisher Scientific, Waltham, MA, USA) medium, supplemented with growth factors and gentamicin in a humidified atmosphere of 95% air/5% CO_2 (*v*/*v*) at 35°C as described.[32] For 6-well and 12-well dishes, each well contained 5 ml and 3 ml F12/DMEM medium, respectively, and these cells were used for specific biochemical assays or for immunoblottings (IB). For single or dual-labeled immunofluorescence analysis (IF), each well (with coverslip) contained 2 ml F12/DMEM. For bicameral units placed in 24-well dishes, the apical and the basal chamber contained 0.5 ml F12/DMEM, supplemented with growth factors and gentamicin.[33] These Sertoli cell cultures were used for experiments on day 2 or 3 with an established functional tight junction (TJ)-permeability barrier, and ultrastructures of TJ, basal ES, gap junction, and desmosome that mimicked the Sertoli cell BTB *in vivo* were also detected by the electron microscopy as earlier described.[34,35]

Overexpression (OE) of pCI-neo/rpS6-WT (wild-type) and pCI-neo/p-rpS6-MT (quadruple phosphomimetic, and constitutively active, mutant [MT]) in primary Sertoli cells cultured in vitro

For rpS6 (rpS6-WT), it was cloned by PCR using primer pairs specific to rpS6 with total cDNAs from Sertoli cells as described.[11] This rpS6 clone was then served as the template to obtain the quadruple phosphomimetic (*i.e.*, constitutively active) mutant (p-rpS6-MT), by site-directed mutagenesis using PCR and corresponding specific primer pairs by converting Ser (S) 235, S236, S240, and S244 to Glu (E) 235, E236, E240, and E244 as described.[11] This rpS6-MT was then cloned into pCI-neo mammalian expression vector.[11,12] Plasmid DNA was obtained using ZymoPURE II Plasmid Kits from Zymo Research (Irvine, CA, USA), wherein endotoxin was also removed as indicated by the manufacturer. For overexpression of pCI-neo/rpS6-WT and pCI-neo/p-rpS6-MT versus empty vector (pCI-neo), Sertoli cells were transfected with the corresponding plasmid DNA (at about 0.45 μg of plasmid DNA per 10^6 Sertoli cells) for 6 h using Lipojet *In Vitro* Transfection Reagent using a 3-μl transfection medium: 1-μg plasmid DNA ratio, according to the manufacturer's protocol as described.[36] Thereafter, transfection reagent was removed and cells were rinsed with sterile PBS (twice). Sertoli cells were incubated with appropriate volume of F12/DMEM with supplements and antibiotics. For cultures to be used for IF, plasmid DNAs were labeled with Label IT® Tracker™ Intracellular Nucleic Acid Localization Cy®3 Kit (Mirus Bio, Madison, WI, USA) (red fluorescence) to track successful transfection as described.[11] Cells were harvested 2 days after transfection with plasmid DNA for fluorescence microscopy and/or preparation of lysates for IB or biochemical analysis for actin or microtubule polymerization assays. Transepithelial electrical resistance (TER) was measured once daily throughout the experimental period to monitor TJ-barrier function.

Assessment of Sertoli cell TJ-permeability barrier function in vitro

The Sertoli cell TJ-permeability barrier function was assessed as described[12,36] using a Millipore Millicell-electrical resistance system (ERS)-2 Volt-ohm meter (MilliporeSigma, St. Louis, MO, USA). Sertoli cells were plated on Matrigel-coated bicameral units (EMD Millipore, Burlington, MA, USA; diameter: 12 mm; pore size: 0.45 μm; effective surface area: 0.6 cm^2) at 1.0×10^6 cells per cm^2. Each bicameral unit was placed inside the well of a 24-well dish with 0.5 ml F12/DMEM each in the apical and the basal compartments. In brief, a short (approximately 2 s) 20-μA pulse of current was sent between the two Ag/AgCl electrodes connected to the ERS meter with each electrode placed in either the apical or basal compartment of the bicameral unit, across the Sertoli cell epithelium (*i.e.*, the Sertoli cell TJ-barrier). The resistance generated by a functional TJ-barrier that blocked the passage of current was then recorded by quantifying the TER in ohms (Ω). In brief, Sertoli cells cultured alone for 3 days were transfected with rpS6-WT and its quadruple constitutively active mutant p-rpS6-MT versus empty vector (*i.e.*, pCI-neo/Ctrl) for overexpression using

approximately 0.45 μg of DNA per 10^6 Sertoli cells for 6 h, and Sertoli cell TJ-permeability barrier function was then monitored daily thereafter by quantifying TER across the cell epithelium. In each experiment, each treatment and control group had triplicate or quadruple bicameral units with a total of three independent experiments using different batches of Sertoli cells, excluding pilot experiments to assess the optimal experimental conditions. Representative data from an experiment were shown, but all experiments yielded similar observations.

IB analysis, IF, F-actin staining, and fluorescence image analysis

IB was performed using corresponding specific antibodies as noted in **Supplementary Table 1.** Fluorescence signal was monitored using home-made chemiluminescent reagents as described.[37] In brief, approximately 20–30 μg protein of Sertoli cell lysates was used for sodium dodecyl sulfate-polyacrylamide gel electrophoresis (SDS-PAGE) and immunoblot analysis. For IF, Sertoli cells cultured on coverslips were fixed in 4% paraformaldehyde (PFA; Sigma-Aldrich, St. Louis, MO, USA) or ice-cold methanol for 10 min, permeabilized in 0.1% Triton X-100 for approximately 5–10 min, blocked in 10% goat serum (*v*/*v*) or 5% bovine serum albumin (BSA) (*w*/*v*) in PBS (10 mmol l^{-1} sodium phosphate, 0.15 mol l^{-1} NaCl, pH 7.4 at 22°C) as described.[38] Thereafter, samples were incubated with the corresponding primary and secondary antibodies (**Supplementary Table 1**), and co-stained with 4′,6-diamidino-2-phenylindole (DAPI, 1 μg ml^{-1}; Sigma-Aldrich) to visualize cell nuclei.[38] Slides were mounted in ProLong™ Diamond Antifade Mountant reagent (Invitrogen/Life Technologies/Thermo Fisher, Waltham, MA, USA). For F-actin staining, Sertoli cells were incubated with Alexa Fluor 488 phalloidin (Invitrogen; green fluorescence) according to the manufacturer's protocols. Images were examined and acquired using a Nikon Eclipse 90i Fluorescence Microscope system equipped with Nikon Ds-Qi1Mc and Nikon DS-Fil digital cameras and Nikon NIS Elements AR 3.2 software (Nikon, Tokyo, Japan). Images were saved in the TIFF format. Image overlays were performed using Adobe Photoshop CS6 (Adobe Systems, San Jose, CA, USA) to assess protein co-localization. All images shown herein were original captured images without further manipulations. Sertoli cells in an experiment, including both control and treatment groups, were analyzed in a single experimental session to avoid inter-experimental variations. Data shown herein were representative micrographs from a single experiment, but each experiment had three coverslips of cells and a total of three independent experiments was performed which yielded similar results. To obtain semi-quantitative data to compare changes in fluorescence intensity in Sertoli cells (*e.g.*, rpS6 fluorescence signal in cells) or at the Sertoli cell-cell interface, the fluorescence signal was quantified using ImageJ software package (version 1.45; http://rsbweb.nih.gov/ij) as earlier described.[8] At least 50 Sertoli cells (or pairs of Sertoli cells to assess changes in protein distribution at the cell-cell interface) were randomly selected and measured from each experimental versus control group from three independent experiments. Immunoblot analysis was also performed as described.[39] To avoid inter-experimental variations, all samples, including both treatment and control groups, were processed simultaneously in a single experimental session.

Actin spin-down assay

The ability of Sertoli cell lysates to polymerize G-actin into F-actin following overexpression of rpS6-WT and p-rpS6-MT versus control (empty) vector was assessed according to the manufacturer's instructions (Cat No. BK037, Cytoskeleton, Denver, CO, USA) as described.[38] In brief, Sertoli cells (approximately 500 μg protein from a single well of a 6-well dish at 0.4×10^6 cells per cm^2) were homogenized in F-actin stabilization buffer, pre-cleared by centrifugation at 350 *g* for 5 min at room temperature to remove cell debris, followed by centrifugation at 100 000 *g* at 37°C for 1 h to separate F-actin from G-actin. Supernatant (approximately 2 ml, containing G-actin) was collected; pellet (containing F-actin) was re-suspended in 300 μl 8 mol l^{-1} urea. Thereafter, 60 μl of supernatant and 60 μl of pellet of each sample were analyzed by immunoblotting for β-actin. Samples from both treatment and control groups in a single experiment were processed simultaneously to avoid inter-experimental variations. Phalloidin (0.1 μmol l^{-1}, actin stabilizing agent) versus urea (80 m mol l^{-1}, actin depolymerization agent) was used as the corresponding positive and negative controls. Data shown herein were from a representative experiment of three independent experiments which yielded similar results.

Actin polymerization assay

Actin polymerization assay was performed as earlier described.[38,40] This assay quantified the ability of Sertoli cell lysates following overexpression of either rpS6-WT or p-rpS6-MT versus empty vector (control) plasmid DNA in Sertoli cells to polymerize pyrene-actin oligomers *in vitro* using kits and protocols from the manufacturer (Cat No. BK003, Cytoskeleton). Assays were performed in Corning 96-well black flat bottom polystyrene microplates (Corning, Lowell, MA, USA). Fluorescence kinetics were monitored from the top in a FilterMax F5 Multi-Mode Microplate Reader and the Multi-Mode Analysis Software 3.4 (Molecular Devices, Sunnyvale, CA, USA) at room temperature (fluorimeter settings used were as follows: measurement type, kinetic, 60 cycle, 60-s interval; excitation wavelength, 360 nm; emission wavelength, 430 nm; integration time, 0.25 ms). Actin polymerization rate assessed by fluorescence intensity increase rate was obtained by linear regression analysis using Microsoft Excel 2013 (Microsoft, Seattle, WA, USA). Phalloidin (1 μmol l^{-1}, an actin-stabilizing agent) versus urea (100 mmol l^{-1}, an actin depolymerization agent) served as the corresponding positive and negative controls. For all the actin assays, the same amount of Sertoli cell lysate (40 μg total protein) from each sample was also analyzed by immunoblot to confirm overexpression of rpS6-WT and p-rpS6-MT. In each experiment, both the treatment and control groups had replicate cultures, and each experiment had three independent experiments using different batches of Sertoli cells which yielded similar results.

Microtubule spin-down assay

This microtubule spin-down assay was performed as described,[41] which estimated the relative level of polymerized microtubules versus free tubulins in Sertoli cell lysates using kits from the cytoskeleton (Cat No. BK038). Taxol (also known as paclitaxel, at 20 μmol l^{-1}, an microtubule-stabilizing agent) and $CaCl_2$ (2 mmol l^{-1}, an microtubule depolymerization agent) served as the corresponding positive and negative controls. In short, this assay assessed changes in the relative distribution of microtubules/polymerized tubulins versus free/nonpolymerized tubulin oligomers in Sertoli cell cytosol.

Statistical analyses

Statistical analysis was performed with GraphPad Prism 6 software (GraphPad Software, San Diego, CA, USA) using either Student's *t*-test (for two-group comparisons), one-way analysis of variance (ANOVA; for multi-group comparisons), or two-way ANOVA with Bonferroni *post hoc* tests. All experiments had 3 to 5 replicate samples with a total of at least three experiments for analysis. $P < 0.5$ was considered as statistically significant.

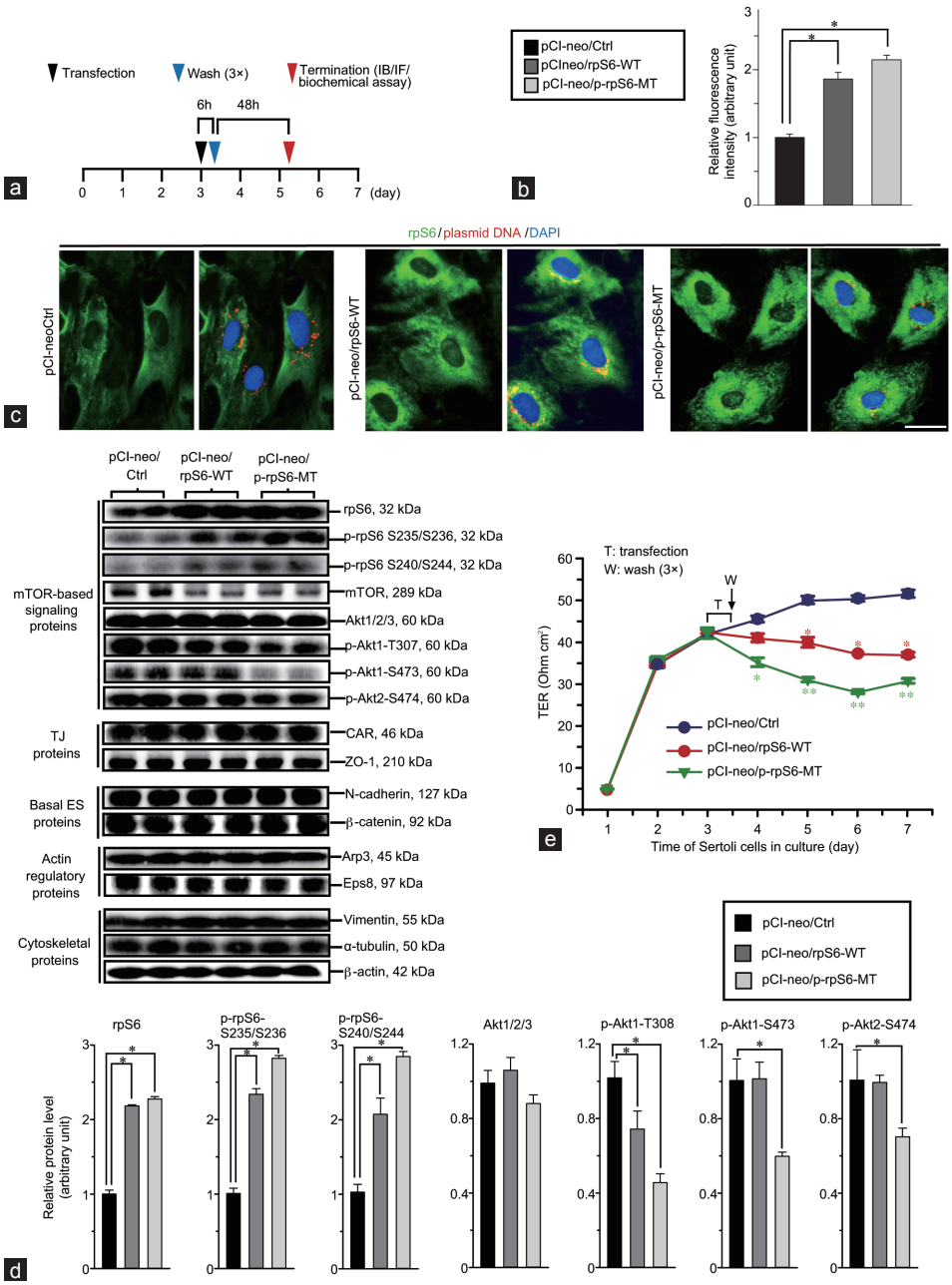

Figure 1: Overexpression of p-rpS6-MT versus rpS6-WT and control (empty) vector in Sertoli cell epithelium with an established TJ-barrier on the Sertoli cell tight junction (TJ)-permeability barrier function. (**a**) Regimen used in this and subsequent experiments reported herein. Data presented herein were results of a representative experiment from three independent experiments, excluding pilot experiments used to establish experimental conditions, using different batches of Sertoli cells, which yielded similar results. (**b**) Composite data of three experiments based on findings shown in **c**, illustrating considerable increase in expression of rpS6 following overexpression of p-rpS6-MT and rpS6-WT versus empty vector in control Sertoli cells when rpS6 (green fluorescence) was quantified. Each bar is a mean ± standard deviation of three experiments. For each experiment, at least 50 Sertoli cells were randomly selected for fluorescence intensity analysis by Image J. $^{*}P < 0.01$, Student's *t*-test by comparing cells from treatment group to control group with the fluorescence intensity of control cells arbitrarily set at 1 for statistical comparison. (**c**) Staining of cells with rpS6 (green fluorescence), red fluorescence represents Cy3-labeled plasmid DNA to confirm successful transfection. Sertoli cell nuclei were visualized by DAPI (blue). Scale bar = 40 μm, which applies to other micrographs in this panel. (**d**) Overexpression of rpS6 (pCI-neo/rpS6-WT) and the constitutively active quadruple phosphomimetic mutant (pCI-neo/p-rpS6-MT) versus controls (emptor vector, pCI-neo/Ctrl) were also confirmed by immunoblot analysis when the protein steady-state levels of rpS6 and its phosphorylated/activated forms were quantified (see bar graphs in the lower panel). A considerable down-regulation of mTOR was noted. Expression of many BTB-associated proteins that were examined was found not to be affected following overexpression of either rpS6-WT or rpS6-MT versus control groups. However, overexpression of rpS6-WT or rpS6-MT led to a down-regulation on the expression of p-Akt1-T307, p-Akt1-S473 and p-Akt2-S474 but not the total Akts (*i.e.*, Akt1/2/3) (bar graphs in lower panel), also consistent with earlier reports.[11,12] Bar graphs on the right panel represent composite data of three experiments. $^{*}P < 0.01$, Student's *t*-test by comparing the treatment with control group wherein protein expression in control group was arbitrarily set at 1 for statistical comparison. **Supplementary Figure 1** for uncropped blots. (**e**) A study to assess changes in the Sertoli cell TJ-permeability barrier function by quantifying transepithelial electrical resistance (TER) across the Sertoli cell epithelium. This is the result of a representation experiment; each data point is the mean ± standard deviation of quadruple bicameral units from three independent experiments using different batches of Sertoli cells. $^{*}P < 0.05$ and $^{**}P < 0.01$, comparing each data point with the corresponding control by Student's *t*-test. DAPI: 4',6-diamidino-2-phenylindole; BTB: blood-testis barrier; mTOR: mammalian target of rapamycin; WT: wild type; Ctrl: control; MT: mutant.

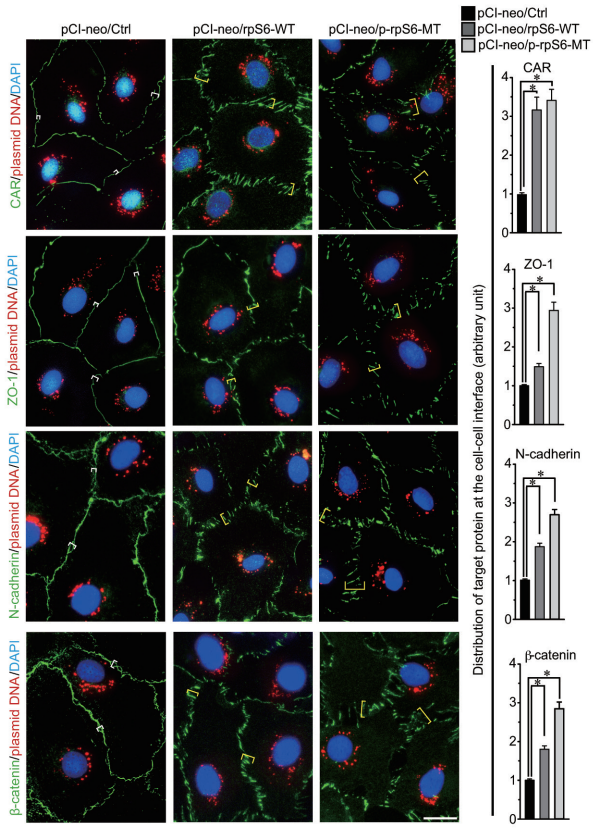

Figure 2: Changes in the distribution of TJ- and basal ES-proteins at the Sertoli cell-cell interface following overexpression of rpS6-WT and p-rpS6-MT versus control cells. Using the regimen shown in **Figure 1a**, overexpression of rpS6-WT or p-rpS6-MT was found to induce changes in the distribution of TJ proteins CAR and ZO-1 (green fluorescence, TJ proteins), and basal ES proteins N-cadherin and β-catenin (green fluorescence, basal ES proteins) at the Sertoli cell-cell interface that constitute the BTB. In control cells overexpressed with pCI-neo empty vector, TJ and basal ES proteins were tightly packed at the cell cortical zone (annotated by white brackets), creating the TJ-permeability barrier as noted in **Figure 1e**. Following overexpression of either rpS6-WT or p-rpS6-MT, these adhesion proteins were rapidly internalized, moving away from the cell-cell interface, apparently being internalized (annotated by yellow brackets). These changes were semi-quantified by measuring the distance of distribution of these proteins at the two opposite ends of adjacent Sertoli cells (see white *vs* yellow brackets), and a total of 80 Sertoli cells were randomly selected and scored of an experiment from three independent experiments using different batches of Sertoli cells. Bar graphs on the right panels are composite data of three experiments, with each bar a mean±standard deviation of these experiments. $^*P < 0.05$, by the Student's *t*-test by comparing cells in treatment groups to control group, which was arbitrarily set at 1 for statistical comparison. It is noted that p-rpS6-MT was more effective to perturb distribution of TJ- and basal ES-proteins. Sertoli cell nuclei were visualized by DAPI staining. Plasmid DNA was labeled with Cy3 (red fluorescence) to confirm successful transfection. Scale bar = 40 μm, which applies to all other micrographs herein. DAPI: 4',6-diamidino-2-phenylindole; CAR: coxsackie and adenovirus receptor; ZO-1: zonula occludens 1; ES: ectoplasmic specialization; BTB: blood-testis barrier; TJ: tight junction; WT: wild type; Ctrl: control; MT: mutant.

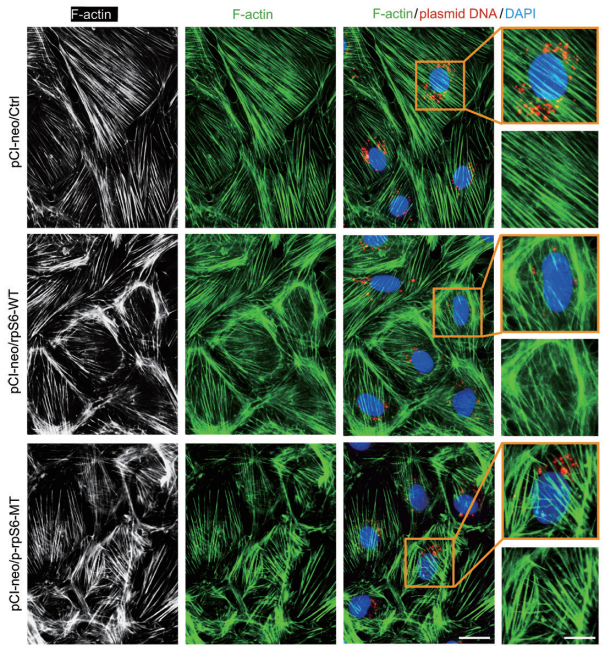

Figure 3: Overexpression of rpS6-WT or p-rpS6-MT in Sertoli cell epithelium perturbs organization of actin filaments across the Sertoli cell cytosol. F-actin in Sertoli cells were visualized by staining with Alexa Fluor 488 phalloidin (green fluorescence, also shown as black-and-white for visualization and comparison). Successful transfection was confirmed by Cy3-labeled plasmid DNA (red fluorescence). Images were also magnified and shown in insets for better visualization. In control cells, actin filaments orderly aligned and stretched across the entire length of Sertoli cell cytosol. Following overexpression of either rpS6-WT or p-rpS6-MT, organization of actin filaments was grossly perturbed. These findings are results of a representative experiment from three independent experiment which yielded similar results. Scale bars = 40 μm; inset, 20 μm; which apply to corresponding micrographs and insets herein. DAPI: 4',6-diamidino-2-phenylindole; Ctrl: control; WT: wild type; MT: mutant.

RESULTS

Overexpression of rpS6 in Sertoli cells affects TJ-permeability barrier function

Sertoli cells cultured *in vitro* alone for 3 days with an established functional TJ-barrier was transfected with different constructs using the mammalian expression vector pCI-neo for overexpression of rpS6-WT (wild type; pCI-neo/rpS6-WT) versus the constitutively active mutant of p-rpS6-MT (pCI-neo/p-rpS6-MT) and empty vector (pCI-neo/Ctrl, served as the control), using the regimen shown in **Figure 1a**. Overexpression of rpS6 in both the rpS6-WT and p-rpS6-MT groups versus the pCI-neo/Ctrl (empty vector) in Sertoli cells was confirmed in **Figure 1b** when the relative fluorescence of rpS6 (green fluorescence) in these cells was assessed (**Figure 1c**). Overexpression of rpS6 in Sertoli cells of the pCI-neo/rpS6-WT and pCI-neo/p-rpS6-MT versus the pCI-neo/Ctrl groups was further confirmed by IB using corresponding antibodies against different phosphorylated forms of rpS6 (**Supplementary Table 1** and **Figure 1d**, also see lower panels for composite data of three independent experiments). Overexpression of rpS6-WT or p-rpS6-MT did not affect many of the BTB-associated proteins examined herein (**Figure 1d**), consistent with earlier reports.[11,12] However, a considerably down-regulation of mTOR was noted (**Figure 1d**), which is also consistent with an earlier report illustrating that a conditional knockout of mTOR in Sertoli cells in a genetic model also led to a surge in the expression of p-rpS6-S240/S244, seminiferous epithelial degeneration and also infertility,[22] consistent with an overexpression of p-rpS6-MT in the testis *in vivo*,[26] and a down-regulation of mTOR as noted herein (**Figure 1d**). Furthermore, overexpression of rpS6-WT was found to perturb the Sertoli cell TJ-barrier function, but the quadruple phosphomimetic (and constitutively active) mutant (*i.e.*, p-rpS6-MT) was more effective than rpS6-WT to perturb the Sertoli cell TJ-barrier function (**Figure 1e**).

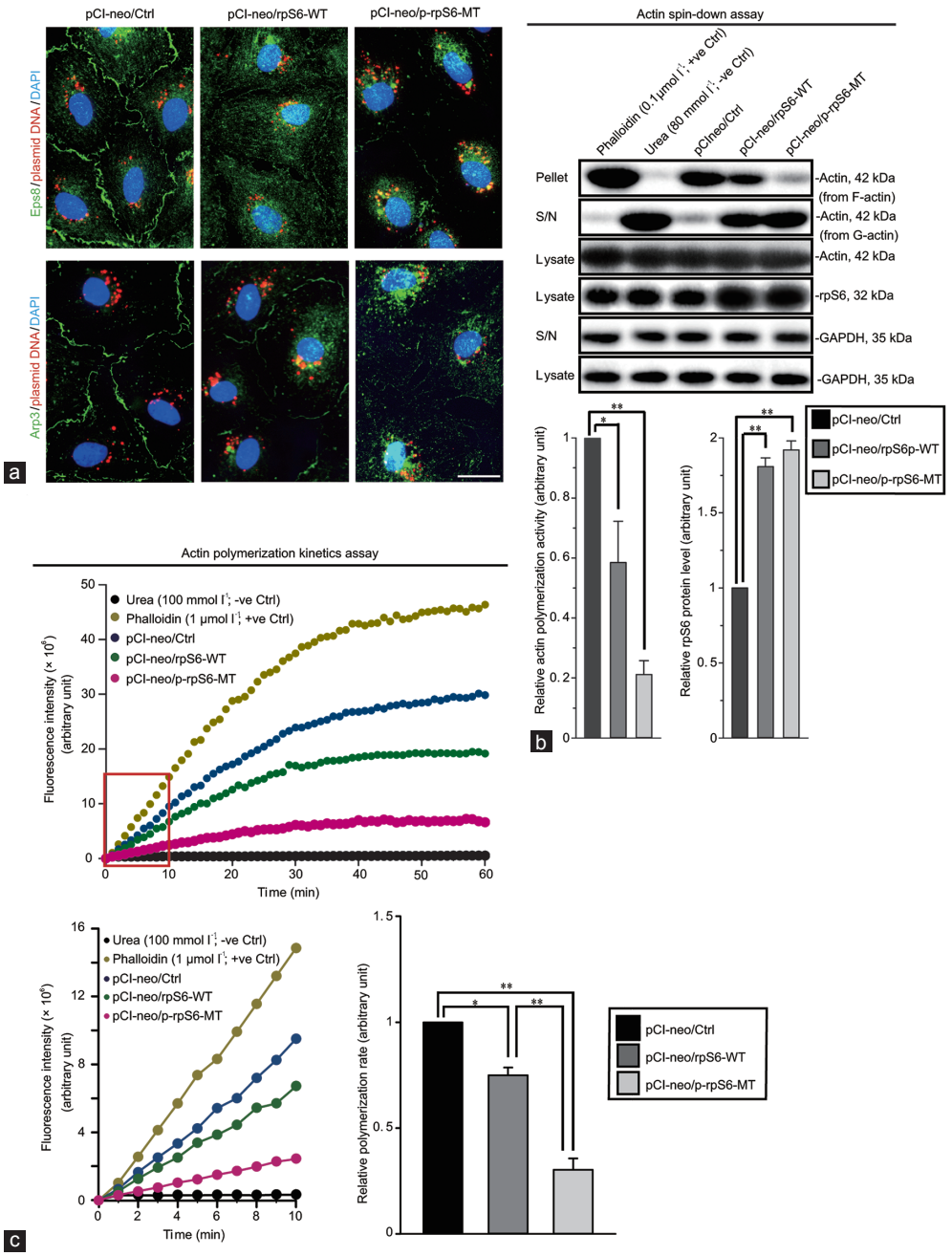

Figure 4: A study to examine the mechanism by overexpression of rpS6-WT or p-rpS6-MT in Sertoli cell epithelium that perturbs actin organization across the Sertoli cell cytosol. (**a**) Overexpression of either rpS6-WT or rpS6-MT perturbs the spatial expression of Eps8 (an actin barbed end capping and bundling protein that confers actin filaments into bundled configuration[59]) and Arp3 (an actin barbed end nucleation protein that induces actin filaments to be organized as a branched network[60]) no longer expressed prominently at the Sertoli cell-cell interface to support actin dynamics to confer the TJ-permeability barrier function. Instead, these proteins were internalized and dispersed in cell cytosol. (**b**) Results of a biochemical spin-down assay that assessed the relative levels of filamentous (F) (*i.e.*, polymerized) actin filaments in pellet versus nonpolymerized globular (G) actin monomers in S/N (supernatant). Each bar of the histograms in the lower panel is a mean ± standard deviation of 3 independent experiments in which statistical comparison was performed between each treatment group and the control group, wherein control (pCI-neo/Ctrl) was arbitrarily set at 1 for statistical comparison. $^{*}P < 0.05$ and $^{**}P < 0.01$, by Student's *t*-test. See uncropped blots in **Supplementary Figure 2**. (**c**) Actin polymerization assay was performed as detailed in Materials and Methods to assess changes in actin polymerization of a representation experiment with triplicate culture dishes. The figure below illustrates the kinetics of actin polymerization during the first 10 min to compare between the treatment and control groups with corresponding +ve and –ve control groups. Each bar is a mean ± standard deviation of three independent experiment in this histogram. $^{*}P < 0.05$ and $^{**}P < 0.01$, by Student's *t*-test. DAPI: 4',6-diamidino-2-phenylindole; MT: mutant; Eps8: epidermal growth factor receptor pathway substrate 8; Arp3: actin-related protein 3; WT: wild type; Ctrl: control.

The disruptive effect of either rpS6-WT or p-rpS6-MT in perturbing the Sertoli cell TJ-barrier function as noted in **Figure 1e** was likely the result of changes in the distribution of adhesion protein complexes at the TJ (*e.g.*, coxsackie and adenovirus receptor [CAR, a TJ integral membrane protein]/zonula occludens 1 [ZO-1, a TJ adaptor protein]) and basal ES (N-cadherin/ β-catenin) at the Sertoli cell-cell interface

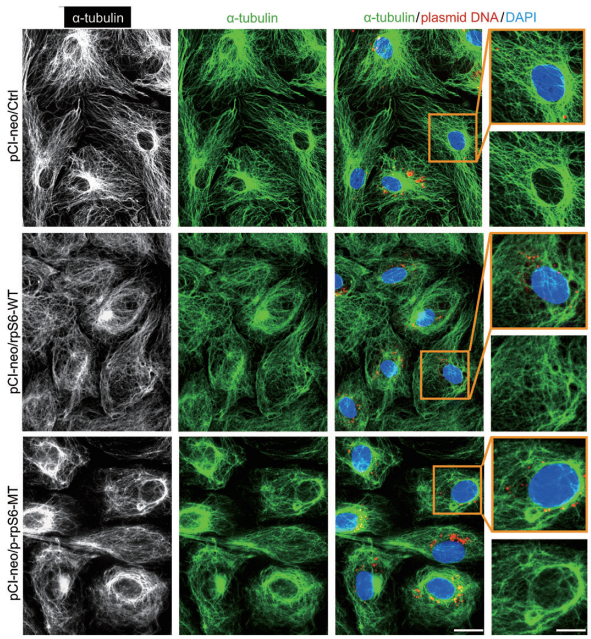

Figure 5: Overexpression of rpS6-WT or p-rpS6-MT in Sertoli cell epithelium perturbs organization of microtubules across the Sertoli cell cytosol. Microtubules, illustrated herein by staining with α-tubulin (green fluorescence), which together with β-tubulin create the α-/β-tubulin oligomers and serve as the building blocks of microtubules. In control cells, microtubules stretched across the Sertoli cell cytosol (the black-and-white micrographs) to support spermatid and cellular transport. Following overexpression of rpS6-WT or rpS6-MT as illustrated by successful transfection using Cy3-labeled plasmid DNA (red fluorescence), microtubules were retracted from cell peripheries and localized closer to the cell nucleus, by wrapping around cell nuclei (stained by DAPI). The net results thus led to failure to support Sertoli cell TJ-permeability barrier function as noted in **Figure 1e**. Micrographs shown herein are representative findings from an experiment of three independent experiments which yielded similar results. Scale bars = 40 μm; inset, 20 μm; which apply to corresponding micrographs and insets as shown herein. DAPI: 4',6-diamidino-2-phenylindole; Ctrl: control; WT: wild type; MT, mutant.

(**Figure 2**). For instance, the CAR/ZO-1 and the N-cadherin/β-catenin protein complexes no longer tightly localized at the cell-cell interface, but moved into the Sertoli cell cytosol (**Figure 2**), thereby failing to support cell adhesive function between Sertoli cells that constitute the BTB, perturbing the TJ-barrier function (**Figure 1e**).

rpS6 regulates actin-based cytoskeletal organization through changes in the spatial expression of actin regulatory proteins and kinetics of actin polymerization

We next examined the underlying mechanism by which overexpression of pCI-neo/rpS6-WT or pCI-neo/p-rpS6- MT (*vs* pCI-neo empty vector) in Sertoli cells perturbed the TJ-barrier function. Specifically, we sought to examine if these changes were mediated through changes in the distribution of adhesion proteins of TJ and/or basal ES. It is noted that these cell adhesion proteins all utilize F-actin for attachments,[14,15] we thus examined any changes in the organization of actin filaments across the Sertoli cell cytosol (**Figure 3**). As expected, overexpression of either pCI-neo/rpS6-WT or pCI-neo/p-rpS6-MT in Sertoli cells perturbed F-actin organization in these cells wherein actin filaments were truncated, as these actin microfilaments no longer aligned orderly and stretched across the entire Sertoli cell as noted in control (pCI-neo/Ctrl) cells (**Figure 3**).

We next examined if these disruptive changes in F-actin organization were the result of changes in actin regulatory proteins, epidermal growth factor receptor pathway substrate 8 (Eps8), and actin-related protein 3 (Arp3) (**Figure 4a**). Eps8 is an actin barbed-end capping and bundling protein,[42,43] conferring actin filaments to a linear and bundled configuration as noted in control cells (**Figure 3**). On the other hand, Arp3 together with Arp2 are known to create the Arp2/3 complex which induces branched actin nucleation protein at the barbed ends, converting linear actin filament to a branched configuration as noted in cells overexpressed with either rpS6-WT or p-rpS6-MT in **Figure 3**. As expected, the spatial expression of these two actin regulatory proteins in Sertoli cell epithelium was considerably disrupted in which they no longer localized prominently at the Sertoli cell-cell interface to confer actin filaments into their bundled configuration to support the TJ-barrier function but randomly dispersed in the cell cytosol (**Figure 4a**). As noted in **Figure 3**, p-rpS6-MT appeared to be more effective than p-rpS6-WT in perturbing F-actin organization versus control (pCI-neo/Ctrl, empty vector) (the enlarged images in insets in **Figure 3** on the right panel). To further confirm if overexpression of the constitutively active p-rpS6-MT in Sertoli cell epithelium is more effective than rpS6-WT to perturb cytoskeletal organization of F-actin, we expanded this work to include an analysis of the actin polymerization activity by assessing the relative ratio between flamentous (F)- and globular (G)-actin (**Figure 4b**) and also the kinetics of actin polymerization (**Figure 4c**). Based on these analyses as noted in the representative findings shown in **Figure 4b**, which illustrated that p-rpS6-MT was more effective than rpS6-WT versus control (pCI-neo/Ctrl, empty vector) (lane 5 *vs* lane 4 and lane 3 in **Figure 4b**, upper panel) to perturb actin polymerization activity in Sertoli cells (composite data of three experiments in the bar graph in the bottom left panel of **Figure 4b**). p-rpS6-MT was also more effective than rpS6-WT to perturb the kinetics of actin polymerization (**Figure 4c**, upper panel), in particular when polymerization kinetics during the first 10 min were further assessed and compared between the treatment and control groups (**Figure 4c**, lower panel) as noted in a representative experiment. This conclusion was also supported by the composite data of three independent experiments shown in **Figure 4c** (the lower right panel).

rpS6 regulates microtubule cytoskeletal organization through changes in the spatial expression EB1 (end binding protein 1, a microtubule plus (+) end tracking protein, +TIP) and microtubule polymerization

Studies have shown that F-actin at the ES is intimately associated with microtubules, and ES is also supported by microtubules structurally and functionally.[14,28,29,44,45] Since rpS6 modulates F-actin organization, we next examined if overexpression of rpS6-WT and p-rpS6-MT would have any effects on microtubule organization in Sertoli cells. As noted in **Figure 5**, microtubules (visualized by α-tubulin staining which, together with β-tubulin, they create the α-/β-tubulin oligo dimers which are the building blocks of microtubules) stretched across the entire Sertoli cell cytosol as distinctive linear fragments (see inserts in control [pCI-neo/Ctrl] cells). However, following overexpression of rpS6-WT in these cells, microtubules were retracted from cell peripheries and concentrated closer to the cell nuclei; and such changes were even more obvious in p-rpS6-MT overexpressed cells wherein microtubules were wrapped around the Sertoli cell nuclei tightly (**Figure 5**).

We next examined changes in the distribution of detyrosinated α-tubulin across the Sertoli cell cytosol, one of the modified forms of tubulins found in mammalian cells. In this context, it is noted that the removal of C-terminal Tyr by exposing Glu at the newly formed C-terminus in detyrosinated α-tubulin is known to induce microtubule stabilization by rendering microtubule less dynamics.[46–48]

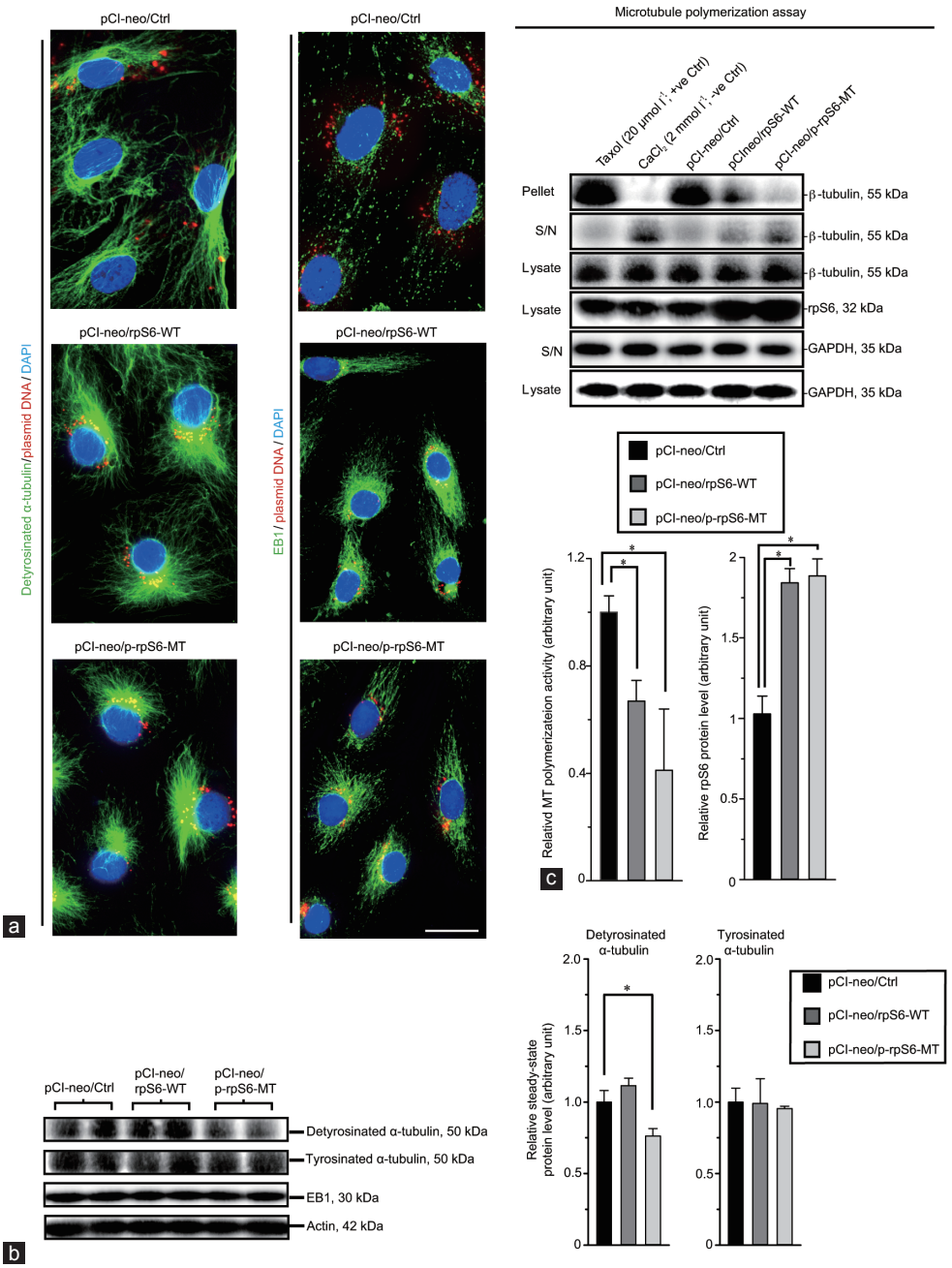

Figure 6: A study to examine the mechanism by which overexpression of rpS6-WT or p-rpS6-MT in Sertoli cell epithelium that perturbs microtubule organization in Sertoli cells. (**a**) Detyrosinated α-tubulin (green fluorescence), a stabilized microtubule form,[49] was found to stretch across the Sertoli cell cytosol in control Sertoli cells. Following overexpression of either rpS6-WT or rpS6-MT, detyrosinated α-tubulin was retracted from cell peripheries and wrapped around the cell nuclei (visualized by DAPI). Cy3-labeled plasmid DNA (red fluorescence) confirmed successful transfection. On the right panel, EB1, a +TIP protein that stabilized microtubules, was also found to localize with microtubules that stretched across the Sertoli cell cytosol in control cells, was retracted from cell peripheries and wrapped around cell nuclei, failing to support microtubules. These are representative micrographs from an experiment of three independent experiments which yielded similar results. Scale bar = 40 μm, which applies to all other micrographs. (**b**) Immunoblot analysis illustrating a mild but consistent down-regulation on the expression of detyrosinated α-tubulin, known to support microtubule stabilization by rendering microtubules less dynamics,[49] following overexpression of either rpS6-WT or rpS6-MT, but it had no effect on the tyrosinated α-tubulin (the less stabilized, more dynamics, form of microtubules[49]). See also uncropped blots in **Supplementary Figure 3a**. (**c**) Results of a biochemical assay that assessed the ability of Sertoli cell lysates following overexpression of rpS6-WT or rpS6-MT to induce microtubule polymerization. Each bar is a mean ± standard deviation of three independent experiments in the histogram shown in the lower panel. These findings thus illustrated overexpression of rpS6-MT was more effective to inhibit microtubule polymerization than rpS6-WT (*vs* control Sertoli cells). Each experiment had triplicate culture wells. $^{*}P < 0.05$, by the Student's *t*-test compared to control group. See also uncropped blots in **Supplementary Figure 3b**. DAPI: 4',6-diamidino-2-phenylindole; MT: mutant; GAPDH: glyceraldehyde-3-phosphate dehydrogenase; Ctrl: control; WT: wild type.

In control cells, detyrosinated α-tubulin stretched across the Sertoli cell cytosol, overexpression of rpS6-WT or p-rpS6-MT caused retraction of detyrosinated α-tubulin from cell peripheries and concentrated closer to the cell nuclei, and considerably more obvious in p-rpS6-MT

overexpressed cells (**Figure 6a**). Furthermore, the steady-state level of detyrosinated α-tubulin, but not tyrosinated α-tubulin (the more dynamics and less stable form of microtubules),[49] were down-regulated in p-rpS6-MT group (but not in rpS6-WT or control group) (**Figure 6b**, left panel; right panel is the composite data) when examined by IB using corresponding specific antibodies (**Supplementary Table 1**). Interestingly, EB1 (a+TIP, known to stabilize microtubules[41,50]) that associated with (+)-end of microtubules that stretched across the Sertoli cell cytosol to support microtubules as noted in control cells were retracted to concentrate closer to the cell nuclei (**Figure 6a**), consistent with findings of microtubule organization noted in **Figure 5**. However, the steady-state protein level of EB1 in both treatment groups was similar to the control group as noted in the immunoblots shown in the lower panel of **Figure 6b**. A biochemical study by assessing the ability of Sertoli cell lysate to polymerize microtubules was also consistent with the fact that overexpression of p-rpS6-MT was considerably more effective than rpS6-WT to perturb microtubule organization by impeding microtubule polymerization (**Figure 6c**). The data shown in the upper panel based on a representative IB experiment was summarized in the bar graph in the lower panel of **Figure 6c**.

DISCUSSION

Findings reported herein have unequivocally demonstrated that overexpression of rpS6, the downstream signaling protein of the mTORC1, exerted its regulatory effects to modulate Sertoli cell function (*e.g.*, TJ-permeability barrier, distribution of adhesive proteins at the cell-cell interface) through changes in the organization of actin- and microtubule-based cytoskeletons. These effects were considerably more pronounced when the quadruple phosphomimetic (*i.e.*, constitutively active) mutant p-rpS6-MT instead of the rpS6-WT was used. Furthermore, overexpression of rpS6 in Sertoli cell epithelium was also shown to down-regulate p-Akt1/2 expression, consistent with earlier reports that a surge in p-rpS6 expression also caused a down-regulation of p-Akt1/2 that led to Sertoli cell dysfunction.[11,12] In short, rpS6 is an integrated component of the mTORC1/rpS6/Akt1/2 signaling pathway that regulates multiple cellular functions based on the studies of mTOR in other epithelia/organs including its role on spermatogenesis in the testis.[2,5,6,51] The fact that the mTOR-based signaling complex regulates spermatogenetic function through actin-based cytoskeleton in rodent testes is consistent with findings based on the use of other study models including genetic models in mice.[22,52,53] For instance, specific deletion of mTOR in Sertoli cells led to progressive testicular atrophy in adult mice and infertility.[22] Phenotypes in the seminiferous epithelium from mice with Sertoli cell-specific knockout of mTOR including the loss of Sertoli cell polarity, increased germ cell apoptosis and sperm abnormalities, germ cell exfoliation due to remarkable disorganization of the seminiferous epithelium, as well as considerable up-regulation on p-rpS6-S240/S244.[22] These findings based on the genetic model thus illustrate that activation of p-rpS6-S240/S244 was associated with disruptive changes in the seminiferous epithelial organization even though the integrity of the actin-based cytoskeleton was not examined in this study, but these mice were found to be infertile.[22] Nonetheless, the notion that mTORC1/rpS6 is involved in the cytoskeletal organization is also supported by a recent study that overexpression of p-rpS6-MT in the testis *in vivo* indeed perturbed the Sertoli cell BTB integrity, which also led to germ cell exfoliation due to disorganization of actin filaments across the seminiferous epithelium.[26]

In addition, specific deletion of Raptor to inactivate mTORC1 in the mouse testis also led to azoospermia and infertility in adult mice due to severe seminiferous tubule degeneration because of extensive disorganization of actin-, microtubule-and vimentin-based cytoskeletons.[53] Furthermore, Sertoli cell-specific knockout of Rictor in the mouse testis that inactivated mTORC2 function also led to azoospermia and these mice were infertile by 3 months of age.[21] A careful examination of the seminiferous epithelium of these mice has shown extensive disorganization of actin- and microtubule-based cytoskeletal organization across the epithelium and a considerable down-regulation of the phosphorylated (activated) form of paxillin.[21] In this context, it is of interest to note that paxillin is a focal adhesion-associated adaptor protein in other epithelial, and it was highly expressed in the ES in the testis to maintain actin cytoskeletal function.[54,55] These findings are also in agreement with an earlier report, illustrating mTOR/Rictor (*i.e.*, mTORC2) complex is crucial to promote Sertoli cell BTB integrity and homeostasis through its effects to promote connexin 43-based GJ function, and also actin-based cytoskeletal organization via PKCα and Rac1 regulatory pathway.[13] Collectively, findings based on the use of genetic models in mice,[22,53] coupled with the data reported herein have provided compelling evidence that mTORC1/rpS6/Akt1/2, besides regulating actin-based cytoskeletal organization, it also modulates microtubule based cytoskeletal organization through changes in the spatial expression of the +TIP protein EB1 and the MT-stabilizing detyrosinated α-tubulin. At present, it remains to be determined if the actin- or the microtubule cytoskeleton (or both) is the primary target of mTORC1/rpS6 signaling complex. Since either actin- or MT-based cytoskeleton is crucial to support endocytic vesicle-mediated protein trafficking,[56–58] an impairment on the function of either the actin or the microtubule cytoskeleton can perturb intracellular protein trafficking, which, in turn, would impede the other cytoskeleton, leading to epithelial dysfunction and degeneration in the testis.

In summary, we demonstrate herein that the mTORC1/rpS6 signaling complex regulates Sertoli cell BTB function via the actin- and microtubule based cytoskeletons, which is mediated through changes in the spatial expression of actin and microtubule regulatory proteins.

AUTHOR CONTRIBUTIONS

CYC conceived the study; CYC, LXL, and SWW designed research; LXL, SWW, MY and CYC performed research; QQL, RSG, and CYC contributed new reagents/analytic tools; LXL, RSG, and CYC performed data analysis; LXL and CYC prepared all figures and wrote the paper; CYC edited the final and prepared revised manuscript. All authors read and approved the final manuscript.

COMPETING INTERESTS

All authors declare no competing interests.

ACKNOWLEDGMENTS

This work was supported in part by grants from the National Institutes of Health (R01 HD056034 to CYC); and the Natural Science Foundation of China (NSFC) (No. 81601264 to LXL; and No. 81730042 to RSG). LXL was also supported by a fellowship from the Wenzhou Medical University.

Supplementary Information is linked to the online version of the paper on the *Asian Journal of Andrology* website.

REFERENCES

1 Laplante M, Sabatini DM. mTOR signaling in growth control and disease. *Cell* 2012; 149: 274–93.
2 Bockaert J, Marin P. mTOR in brain physiology and pathologies. *Physiol Rev* 2015; 95: 1157–87.
3 Long X, Muller F, Avruch J. TOR action in mammalian cells and in *Caenorhabditis*

elegans. *Curr Top Microbiol Immunol* 2004; 279: 115–38.
4 Shimobayashi M, Hall MN. Making new contacts: the mTOR network in metabolism and signalling crosstalk. *Nat Rev Mol Cell Biol* 2014; 15: 155–62.
5 Li N, Cheng CY. Mammalian target of rapamycin complex (mTOR) pathway modulates blood-testis barrier (BTB) function through F-actin organization and gap junction. *Histol Histopathol* 2016; 31: 961–8.
6 Mok KW, Mruk DD, Cheng CY. Regulation of blood-testis barrier (BTB) dynamics during spermatogenesis via the "Yin" and "Yang" effects of mammalian target of rapamycin complex 1 (mTORC1) and mTORC2. *Int Rev Cell Mol Biol* 2013; 301: 291–358.
7 Wullschleger S, Loewith R, Hall MN. TOR signaling in growth and metabolism. *Cell* 2006; 124: 471–84.
8 Mok KW, Mruk DD, Silvestrini B, Cheng CY. rpS6 regulates blood-testis barrier dynamics by affecting F-actin organization and protein recruitment. *Endocrinology* 2012; 153: 5036–48.
9 Meyuhas O. Ribosomal protein S6 phosphorylation: four decades of research. *Int Rev Cell Mol Biol* 2015; 320: 41–73.
10 Meyuhas O, Dreazen A. Ribosomal protein S6 kinase from TOP mRNAs to cell size. *Prog Mol Biol Transl Sci* 2009; 90: 109–53.
11 Mok KW, Mruk DD, Cheng CY. rpS6 regulates blood-testis barrier dynamics through Akt-mediated effects on MMP-9. *J Cell Sci* 2014; 127: 4870–82.
12 Mok KW, Chen H, Lee WM, Cheng CY. rpS6 regulates blood-testis barrier dynamics through Arp3-mediated actin microfilament organization in rat Sertoli cells. An *in vitro* study. *Endocrinology* 2015; 156: 1900–13.
13 Mok KW, Mruk DD, Lee WM, Cheng CY. Rictor/mTORC2 regulates blood-testis barrier dynamics via its effects on gap junction communications and actin filament network. *FASEB J* 2013; 27: 1137–52.
14 Vogl AW, Vaid KS, Guttman JA. The Sertoli cell cytoskeleton. *Adv Exp Med Biol* 2008; 636: 186–211.
15 Cheng CY, Mruk DD. Cell junction dynamics in the testis: Sertoli-germ cell interactions and male contraceptive development. *Physiol Rev* 2002; 82: 825–74.
16 Mruk DD, Cheng CY. Sertoli-Sertoli and Sertoli-germ cell interactions and their significance in germ cell movement in the seminiferous epithelium during spermatogenesis. *Endocr Rev* 2004; 25: 747–806.
17 Pelletier RM. The blood-testis barrier: the junctional permeability, the proteins and the lipids. *Prog Histochem Cytochem* 2011; 46: 49–127.
18 Mital P, Hinton BT, Dufour JM. The blood-testis and blood-epididymis barriers are more than just their tight junctions. *Biol Reprod* 2011; 84: 851–8.
19 Li MW, Mruk DD, Lee WM, Cheng CY. Connexin 43 and plakophilin-2 as a protein complex that regulates blood-testis barrier dynamics. *Proc Natl Acad Sci USA* 2009; 106: 10213–8.
20 Li MW, Mruk DD, Lee WM, Cheng CY. Connexin 43 is critical to maintain the homeostasis of blood-testis barrier via its effects on tight junction reassembly. *Proc Natl Acad Sci USA* 2010; 107: 17998–8003.
21 Dong H, Chen Z, Wang C, Xiong Z, Zhao W, *et al*. Rictor regulates spermatogenesis by controlling Sertoli cell cytoskeletal organization and cell polarity in the mouse testis. *Endocrinology* 2015; 156: 4244–56.
22 Boyer A, Girard M, Thimmanahalli DS, Levasseur A, Celeste C, *et al*. mTOR regulates gap junction alpha-1 protein trafficking in Sertoli cells and is required for the maintenance of spermatogenesis in mice. *Biol Reprod* 2016; 95: 13.
23 Schell C, Kretz O, Liang W, Kiefer B, Schneider S, *et al*. The rapamycin-sensitive complex of mammalian target of rapamycin is essential to maintain male fertility. *Am J Pathol* 2016; 186: 324–36.
24 Serra ND, Velte EK, Niedenberger BA, Kirsanov O, Geyer CB. Cell-autonomous requirement for mammalian target of rapamycin (Mtor) in spermatogonial proliferation and differentiation in the mousedagger. *Biol Reprod* 2017; 96: 816–28.
25 Bai S, Cheng L, Zhang Y, Zhu C, Zhu Z, *et al*. A germline-specific role for the mTORC2 component rictor in maintaining spermatogonial differentiation and intercellular adhesion in mouse testis. *Mol Hum Reprod* 2018; 24: 244–59.
26 Li SY, Yan M, Chen H, Jesus TT, Lee WM, *et al*. mTORC1/rpS6 regulates blood-testis barrier (BTB) dynamics and spermatogenetic function in the testis *in vivo*. *Am J Physiol Endocrinol Metab* 2018; 314: E174–90.
27 Vogl A, Pfeiffer D, Redenbach D. Ectoplasmic ("junctional") specializations in mammalian Sertoli cells: influence on spermatogenic cells. *Ann N Y Acad Sci* 1991; 637: 175–202.
28 Russell LD, Peterson RN. Sertoli cell junctions: morphological and functional correlates. *Int Rev Cytol* 1985; 94: 177–211.
29 Tang EI, Mruk DD, Cheng CY. Regulation of microtubule (MT)-based cytoskeleton in the seminiferous epithelium during spermatogenesis. *Semin Cell Dev Biol* 2016; 59: 35–45.
30 Redenbach DM, Vogl AW. Microtubule polarity in Sertoli cells: a model for microtubule-based spermatid transport. *Eur J Cell Biol* 1991; 54: 277–90.
31 Redenbach DM, Boekelheide K. Microtubules are oriented with their minus-ends directed apically before tight junction formation in rat Sertoli cells. *Eur J Cell Biol* 1994; 65: 246–57.
32 Mruk DD, Cheng CY. An *in vitro* system to study Sertoli cell blood-testis barrier dynamics. *Methods Mol Biol* 2011; 763: 237–52.
33 Mruk DD, Cheng CY. Testin and actin are key molecular targets of adjudin, an anti-spermatogenic agent, in the testis. *Spermatogenesis* 2011; 1: 137–46.
34 Lie PP, Cheng CY, Mruk DD. Crosstalk between desmoglein-2/desmocollin-2/Src kinase and coxsackie and adenovirus receptor/ZO-1 protein complexes, regulates blood-testis barrier dynamics. *Int J Biochem Cell Biol* 2010; 42: 975–86.
35 Li MW, Mruk DD, Lee WM, Cheng CY. Disruption of the blood-testis barrier integrity by bisphenol A *in vitro*: is this a suitable model for studying blood-testis barrier dynamics? *Int J Biochem Cell Biol* 2009; 41: 2302-14.
36 Gao Y, Mruk D, Chen H, Lui WY, Lee WM, *et al*. Regulation of the blood-testis barrier by a local axis in the testis: role of laminin α2 in the basement membrane. *FASEB J* 2017; 31: 584–97.
37 Mruk DD, Cheng CY. Enhanced chemiluminescence (ECL) for routine immunoblotting. An inexpensive alternative to commercially available kits. *Spermatogenesis* 2011; 1: 121–2.
38 Wen Q, Li N, Xiao X, Lui WY, Chu DS, *et al*. Actin nucleator Spire 1 is a regulator of ectoplasmic specialization in the testis. *Cell Death Dis* 2018; 9: 208.
39 Li L, Tang EI, Chen H, Lian Q, Ge R, *et al*. Sperm release at spermiation is regulated by changes in the organization of actin- and microtubule-based cytoskeletons at the apical ectoplasmic specialization – a study using the adjudin model. *Endocrinology* 2017; 158: 4300–16.
40 Li N, Mruk DD, Wong CK, Lee WM, Han D, *et al*. Actin-bundling protein plastin 3 is a regulator of ectoplasmic specialization dynamics during spermatogenesis in the rat testis. *FASEB J* 2015; 29: 3788–805.
41 Tang EI, Mok KW, Lee WM, Cheng CY. EB1 regulates tubulin and actin cytoskeletal networks at the Sertoli cell blood-testis barrier in male rats – an *in vitro* study. *Endocrinology* 2015; 156: 680–93.
42 Ahmed S, Goh WI, Bu W. I-BAR domains, IRSp53 and filopodium formation. *Semin Cell Dev Biol* 2010; 21: 350–6.
43 Cheng CY, Mruk DD. Regulation of spermiogenesis, spermiation and blood-testis barrier dynamics: novel insights from studies on Eps8 and Arp3. *Biochem J* 2011; 435: 553–62.
44 Russell L. Sertoli-germ cell interrelations: a review. *Gamete Res* 1980; 3: 179–202.
45 Redenbach D, Boekelheide K, Vogl A. Binding between mammalian spermatid-ectoplasmic specialization complexes and microtubules. *Eur J Cell Biol* 1992; 59: 433–48.
46 Infante AS, Stein MS, Zhai Y, Borisy GG, Gundersen GG. Detyrosinated (Glu) microtubules are stabilized by an ATP-sensitive plus-end cap. *J Cell Sci* 2000; 113: 3907–19.
47 Dunn S, Morrison E, Liverpool TB, Molina-Paris C, Cross RA, *et al*. Differential trafficking of Kif5c on tyrosinated and detyrosinated microtubules in live cells. *J Cell Sci* 2008; 121: 1085–95.
48 Kreis TE. Microtubules containing detyrosinated tubulin are less dynamic. *EMBO J* 1987; 6: 2597–606.
49 Janke C. The tubulin code: molecular components, readout mechanisms, and functions. *J Cell Biol* 2014; 206: 461–72.
50 Akhmanova A, Steinmetz MO. Microtubule +TIPs at a glance. *J Cell Sci* 2010; 123: 3415–9.
51 Jewell JL, Russell RC, Guan KL. Amino acid signalling upstream of mTOR. *Nat Rev Mol Cell Biol* 2013; 14: 133–9.
52 Tsuji-Tamura K, Ogawa M. Dual inhibition of mTORC1 and mTORC2 perturbs cytoskeletal organization and impairs endothelial cell elongation. *Biochem Biophys Res Commun* 2018; 497: 326–31.
53 Xiong Z, Wang C, Wang Z, Dai H, Song Q, *et al*. Raptor directs Sertoli cell cytoskeletal organization and polarity in the mouse testis. *Biol Reprod* 2018; 99: 1289–302.
54 Mulholland DJ, Dedhar S, Vogl AW. Rat seminiferous epithelium contains a unique junction (ectoplasmic specialization) with signaling properties both of cell/cell and cell/matrix junctions. *Biol Reprod* 2001; 64: 396–407.
55 Siu MK, Mruk DD, Lee WM, Cheng CY. Adhering junction dynamics in the testis are regulated by an interplay of b1-integrin and focal adhesion complex (FAC)-associated proteins. *Endocrinology* 2003; 144: 2141–63.
56 Granger E, McNee G, Allan V, Woodman P. The role of the cytoskeleton and molecular motors in endosomal dynamics. *Semin Cell Dev Biol* 2014; 31: 20–9.
57 Kim K, Gadila SK. Cargo trafficking from the trans-Golgi network towards the endosome. *Biol Cell* 2016; 108: 205–18.
58 Gautreau A, Oguievetskaia K, Ungermann C. Function and regulation of the endosomal fusion and fission machineries. *Cold Spring Harb Perspect Biol* 2014; 6: a016832.
59 Lie PP, Mruk DD, Lee WM, Cheng CY. Epidermal growth factor receptor pathway substrate 8 (Eps8) is a novel regulator of cell adhesion and the blood-testis barrier integrity in the seminiferous epithelium. *FASEB J* 2009; 23: 2555–67.
60 Lie PP, Chan AY, Mruk DD, Lee WM, Cheng CY. Restricted Arp3 expression in the testis prevents blood-testis barrier disruption during junction restructuring at spermatogenesis. *Proc Natl Acad Sci U S A* 2010; 107: 11411–6.

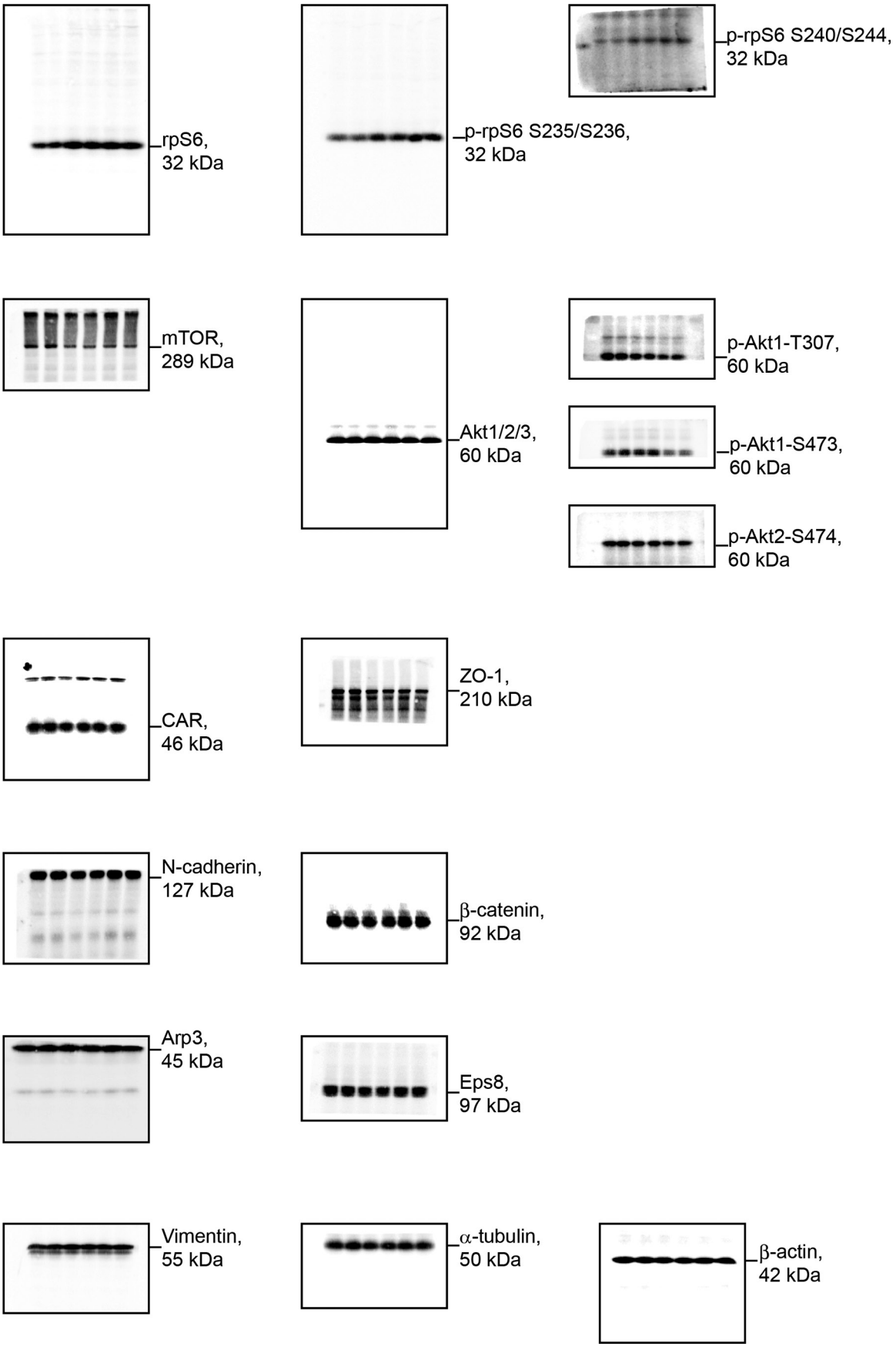

Supplementary Figure 1: Uncropped blots correspond to immunoblot data shown in **Figure 1d**.

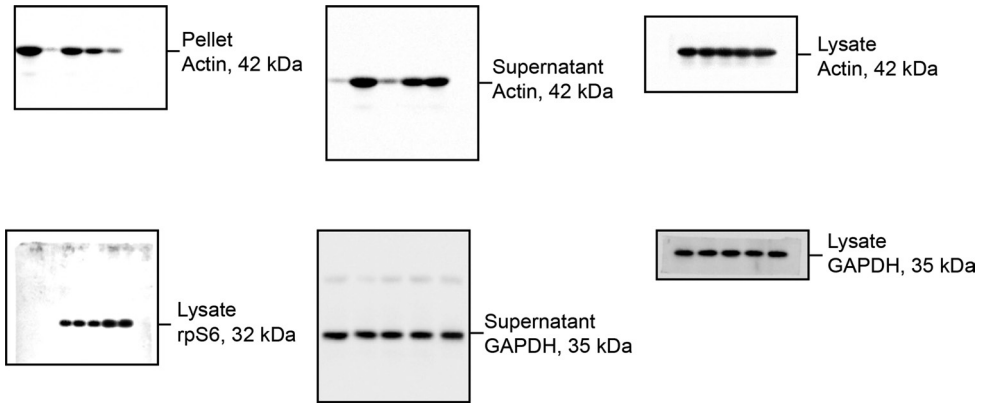

Supplementary Figure 2: Uncropped blots correspond to immunoblot data shown in **Figure 4b**.

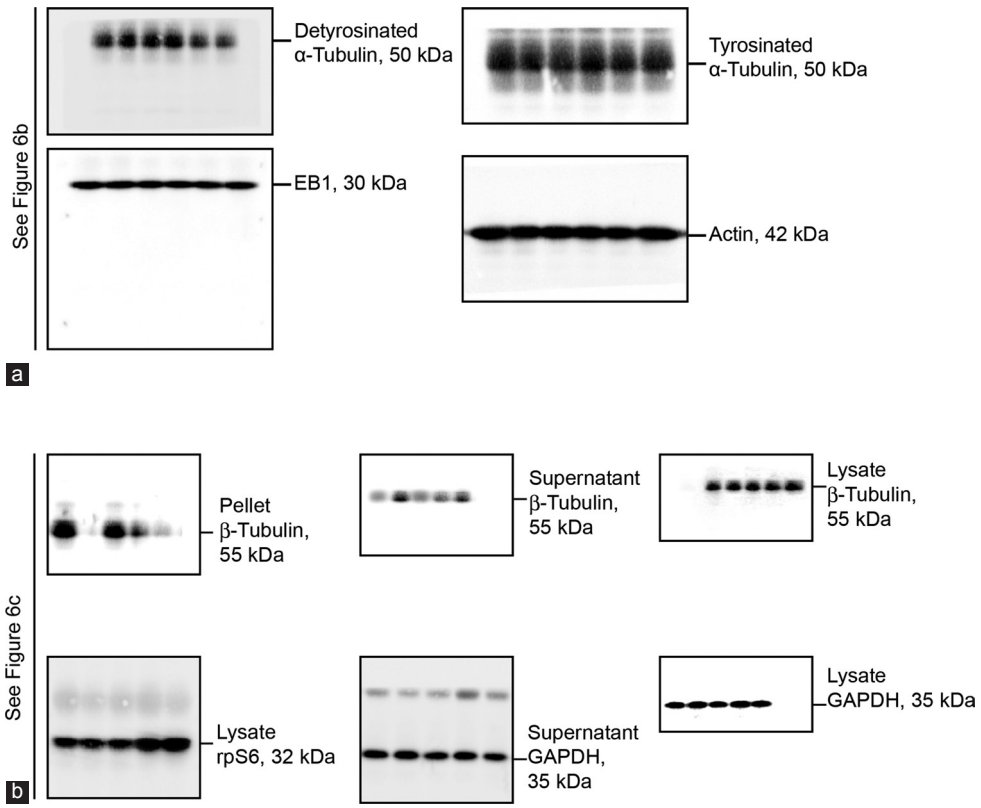

Supplementary Figure 3: Uncropped blots of (**a**) and (**b**) corresponding to immunoblot data shown in **Figure 6b** and **6c**.

SUPPLEMENTARY TABLE

Table S1. Antibodies used for all experiments in this report

Antibody (RRID Number*)	Host Species	Vendor	Catalog Number	Working Dilution	
				IB	IF
rpS6 (AB_331355)	Rabbit	Cell Signaling Technology (Danvers, MA)	2217	1:1000	1:100
p-rpS6 S235/S236 (AB_916156)	Rabbit	Cell Signaling Technology	4858	1:2000	
p-rpS6 S240/S244 (AB_10694233)	Rabbit	Cell Signaling Technology	5364	1:1000	
Arp3 (AB_476749)	Mouse	Sigma-Aldrich (St Louis, MO)	A5979	1:3000	1:200
Eps8 (AB_397544)	Mouse	Thermo Fisher Scientific (Waltham, MA)	610143	1:5000	1:100
EB1 (AB_2141629)	Rabbit	Santa Cruz Biotechnology (Dallas, TX)	sc-15347	1:200	1:300
α-tubulin (AB_2241126)	Mouse	Abcam (Cambridge, MA)	ab7291	1:1000	1:200
β-tubulin (AB_2210370)	Rabbit	Abcam	ab6046	1:1000	
Detyrosinated α-tubulin (AB_869990)	Rabbit	Abcam	ab48389	1:1000	1:200
Tyrosinated α-tubulin (AB_261811)	Mouse	Sigma-Aldrich	T9028	1:1000	
Akt1/2/3 (AB_329827)	Rabbit	Cell Signaling Technology	9272	1:1000	
Phospho-Akt1 (Thr308) (AB_2255933)	Rabbit	Cell Signaling Technology	2965	1:1000	
Phospho-Akt1 (Ser473) (AB_2629283)	Rabbit	Cell Signaling Technology	9018	1:1000	
Phospho-Akt2 (Ser474) (AB_2630347)	Rabbit	Cell Signaling Technology	8599	1:1000	
Vimentin (AB_628437)	Mouse	Santa Cruz Biotechnology	sc-6260	1:200	
β-Actin (AB_2714189)	Mouse	Santa Cruz Biotechnology	sc-47778	1:500	
GAPDH (AB_2107448)	Mouse	Abcam	ab8245	1:1000	
mTOR (AB_2105622)	Rabbit	Cell Signaling Technology	2983	1:2000	
CAR (AB_2087557)	Rabbit	Santa Cruz Biotechnology	sc-15405	1:200	1:50
ZO-1 (AB_2533938)	Rabbit	Thermo Fisher Scientific	61–7300	1:250	1:100
N-cadherin (AB_647794)	Rabbit	Santa Cruz Biotechnology	sc-7939	1:200	

N-cadherin (AB_2313779)	Mouse	Thermo Fisher Scientific	33–3900		1:100
β-catenin (AB_634603)	Rabbit	Santa Cruz Biotechnology	sc-7199	1:250	
β-catenin (AB_2533982)	Rabbit	Thermo Fisher Scientific	71–2700		1:100
Goat anti-Rabbit IgG-HRP (AB_2534776)	Goat	Thermo Fisher Scientific	A16104	1:20000	
Goat anti-Mouse IgG-HRP (AB_2534745)	Goat	Thermo Fisher Scientific	A16072	1:10000	
Bovine anti-Goat IgG-HRP (AB_634811)	Bovine	Santa Cruz Biotechnology	sc-2350	1:3000	
Rabbit IgG-Alexa Fluor 488 (AB_2576217)	Goat	Thermo Fisher Scientific	A-11034		1:250
Mouse IgG-Alexa Fluor 488 (AB_2534088)	Goat	Thermo Fisher Scientific	A-11029		1:250

*Abbreviations used: Arp3, actin-related protein 3, which together with Arp2 create the Arp2/3 complex known to induced branched actin polymerization, converting linear actin filaments into a branched network; CAR, coxsackievirus and adenovirus receptor, a TJ integral membrane protein; EB1, end-binding 1 protein, a microtubule plus (+)-end tracking protein, or +TIP; Eps8, epidermal growth factor receptor pathway substrate 8, an actin barbed end capping and bundling protein; mTOR, mammalian target of rapamycin, a Ser/Thr protein kinase known to regulate cellular energy and multiple cellular events in mammalian cells; rpS6, ribosomal protein S6, a downstream signaling protein, also a Ser/Thr protein kinase, of mTORC1; ZO-1; zonula occludens-1.